Available online at www.sciencedirect.com
ScienceDirect
Desalination 243 (2009) 170–181
DESALINATION
www.elsevier.com/locate/desal

Separation of dimethyl phenol using a spiral-wound RO membrane — Experimental and parameter estimation studies

G. Srinivasan[a*], S. Sundaramoorthy[a], D.V.R. Murthy[b]
[a]*Department of Chemical Engineering, Pondicherry Engineering College, Puducherry, India*
Tel. +91 9442215600; Fax: +91 413 265-5101; email: seenu_pec@yahoo.com
[b]*Department of Chemical Engineering, National Institute of Technology, Karnataka, Surathkal, India*

Received 25 October 2007; Accepted 13 April 2008

Abstract

Reverse osmosis (RO) is increasingly used as a separation technique in chemical and environmental engineering for the removal of organics and organic pollutants present in waste water. Treatment of organics by RO is dependent on many factors and hence developing a viable RO system involves extensive pilot-plant studies. The removal of an organic compound, namely dimethyl phenol, using a polyamide membrane was investigated in this study. Experiments were conducted on a laboratory-scale spiral-wound RO module. The permeate concentrations and rejection coefficient values were measured for various transmembrane pressures and feed concentrations. A maximum rejection of 97% was observed. A mathematical model was developed for the RO module assuming a solution–diffusion mechanism for solute and solvent transport through the membrane and considering the concentration and pressure to be uniform on both permeate and retentate sides. The model has four parameters. A graphical method for estimating the model parameters was proposed. The model and the estimated parameter values were validated with the experimental data. The model was able to predict the permeate concentration within an error of 19% and rejection within 2% error.

Keywords: Reverse osmosis; Polyamide membrane; Spiral-wound module; Dimethyl phenol

1. Introduction

The applicability of membrane separation processes for the treatment of hazardous, complex, aqueous industrial wastes are well known. Reverse osmosis (RO) has been widely used for the desalination of seawater, brackish water and the treatment of industrial effluents [1–3]. The removal of organic and toxic contaminants by selective transport through membrane is of wide spread applicability and is beginning to be used on a large scale. In the waste water treatment

*Corresponding author.

0011-9164/09/$– See front matter
doi:10.1016/j.desal.2008.04.023

using RO process, the toxic contaminant gets concentrated into a small fraction of the total waste volume facilitating further treatment.

A number of studies on the use of RO for the treatment of organics and inorganic solutes are reported in the literature. Applications of RO in the treatment of effluents from the chemical, textile, petrochemical, electrochemical, pulp and paper and food industries have been reviewed by Slater et al. [4]. Shuckrow et al. [5,6] have conducted studies on the treatment of industrial waste water and reported a rejection of 50%, 10% and 25% respectively for organic contaminants namely phenol, benzene and methylene chloride and 30%, 92%, 42% and 25% respectively for inorganic pollutants namely antimony, arsenic, cyanide, lead. The removal of specific contaminants like pesticides, antibiotics, endocrine-disrupting compounds and pharmaceutically active compounds were studied by many authors [7–10]. These studies have revealed that the efficiency as well as the mechanism of rejection of organic solutes by membranes are influenced by various operating parameters like pressure, concentration, flow rate, membrane sieving effect, membrane solute interactions, physico-chemical properties of solute (acidity, polarity, solute radius) and membrane type. Due to the influence of above listed variables, developing a viable RO operating system for separation of organic compounds involves extensive laboratory studies.

The separation of phenolic compounds using RO is of practical interest in the context of industrial effluent treatment. A number of studies on the removal of aromatics like phenol, chlorophenol, and alkyl phenols, have been reported in the literature [11–18]. In this work, a phenolic compound, dimethyl phenol, was studied for its removal using RO. Dimethyl phenol is an important organic aromatic compound that occurs in waste water from various industrial activities such as petroleum processing, plastic manufacturing and the production of resins. It is considered to be a toxic compound by the Agency for Toxic Substances & Disease Registry and even low concentrations of this compound are hazardous because of its toxicity to animal, plant and human life.

Models that adequately describe the performance of RO membranes play a very significant role in the design of RO processes. Many mechanistic and mathematical models have been proposed to describe RO membranes. Two of the widely used models that describe the transport through the RO membrane are the solution diffusion model proposed by Lonsdale [19] and the irreversible thermodynamics model proposed by Kedem and Spiegler [20]. These models could be used to predict the solute and solvent transport characteristics of the membranes with reasonable success. Excellent critical reviews of these transport models are available in the literature [21–25].

Of all the modular designs of RO units, the spiral-wound module is widely used due to its large area to volume ratio. A number of models are proposed in the literature [26,27] for predicting the performance of spiral-wound modules. Many of the models that consider spatial variation of parameters like pressure, concentration and flow rates on permeate and retentate sides require rigorous numerical solutions. [28,29]. Hence, most of the modeling and parameter estimation studies reported on spiral-wound modules [30,31] neglect the spatial variation of the above parameters and assume the parameters to be uniform throughout the permeate and retentate sides. This lumped parameter model for the spiral-wound RO module is adequate for small size modules.

In the present study, the separation efficiency of a spiral-wound RO process in removing 2,4-dimethyl phenol from a synthetic aqueous binary solution was investigated. Experiments on a laboratory-scale spiral-wound RO unit were conducted by measuring concentration and flow rates of permeate and retentate for various transmembrane pressure and feed concentrations. The total

feed flow rate was not varied. A mathematical model was developed for the RO module assuming a solution–diffusion mechanism for solute and solvent transport through the membrane and considering the concentration and pressure on both permeate and retentate sides to be uniform. (lumped parameter model). The model had four parameters which were estimated by a graphical method using the experimental data. For estimating two of the four model parameters, the method proposed by Murthy and Gupta [30] was used and for estimating the other two parameters, a new graphical method was proposed in this work. The estimated model parameters were validated using the experimental data.

2. Experimental

2.1. Experimental set-up

The Perma-TFC polyamide RO membrane in spiral-wound configuration (supplied by Permionics, Vadodara, India) was used in this study. Details about the size and the geometry of the module are given in Table 1. The experimental set-up shown in Fig. 1 consisted of a membrane module kept inside a stainless steel cylindrical housing, a feed tank, retentate and permeate collection tanks. A high pressure pump (P) capable of developing a pressure up to 20 atm (300 psi) pumps the feed liquid through the membrane system at a fixed flow rate of 20 LPM. A micron filter installed in the upstream side of the membrane unit prevents entry of suspended solid particles which otherwise would damage the membrane. A manual needle valve (v3) was provided at the outlet of the retentate line to pressurize the feed liquid to a desired pressure indicated by pressure gauges installed in the feed and retentate lines. The permeate and the concentrate flow rates were measured by means of rotameters. A HPLC (Perkin Elmer, USA) equipped with a UV detector and C-18 column was used for the analysis and measurement of dimethyl phenol concentration in retentate and permeate samples.

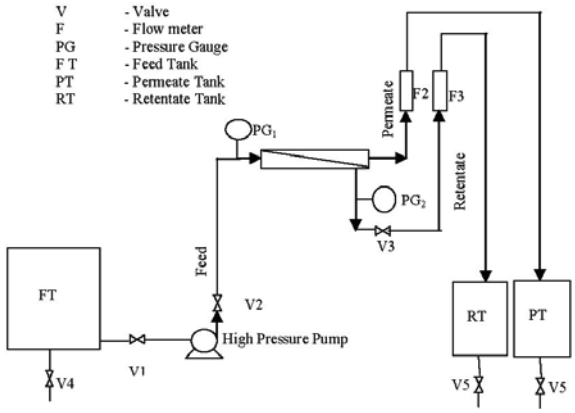

Fig. 1. Schematic diagram of the experimental set-up.

Table 1
Specification of polyamide membrane module

Membrane module	Spiral wound
Number of turns (n)	13
Feed spacer thickness (t_f), mm	0.78
Permeate channel thickness (t_p), mm	0.85
Membrane area (A_M) , m^2	0.75
Module length (L), m	0.45
Module diameter (D), "	2.5

2.2. Experimental methods

Feed solutions containing specific ppm of dimethyl phenol in water were prepared by dissolving weighed quantities of dimethyl phenol in raw water and taken in feed tank. The feed was pumped at a fixed flow rate of 20 LPM. The feed pressure to the membrane module was varied in the range of 2–13 atm using the manual valve provided at the module outlet and the pressure gauge readings at the feed inlet and retentate outlet were recorded. Feed temperature was the ambient temperature that was read using a thermometer provided in the feed tank. The permeate and retentate flow rates read by rotameters were

Table 2
Experimental data obtained for the dimethyl phenol–water system using a RO polyamide membrane

Set no.	Pressure (atm)		Temp.	$C_i\times10^{+3}$	$C_p\times10^{+4}$	$C_o\times10^{+3}$	$F_p\times10^{+6}$	$F_o\times10^{+4}$	$J_v\times10^{+6}$	R_{exp}
	Pi	*Po*	°C	(kmol/m^3)	(kmol/m^3)	(kmol/m^3)	(m^3/s)	(m^3/s)	(m/s)	
1	4.90	1.47	32	0.69	0.486	0.696	3.46	3.29	4.61	0.930
2	6.86	3.43	34	0.69	0.402	0.698	4.86	3.28	6.48	0.942
3	7.84	4.41	35	0.69	0.389	0.694	6.16	3.27	8.21	0.943
4	9.80	6.37	35	0.69	0.379	0.691	7.80	3.25	10.40	0.945
5	11.76	8.33	35	0.69	0.348	0.696	9.60	3.23	12.80	0.950
6	4.90	1.47	35	1.43	1.150	1.530	3.28	3.30	4.37	0.924
7	6.86	3.43	36	1.43	1.070	1.540	5.05	3.28	6.73	0.930
8	7.84	4.41	37	1.43	0.890	1.530	6.08	3.27	8.11	0.941
9	9.80	6.37	37	1.43	0.760	1.540	7.75	3.25	10.33	0.950
10	11.76	8.33	37	1.43	0.750	1.550	9.43	3.24	12.57	0.951
11	4.90	1.47	37	2.52	1.950	2.540	3.41	3.29	4.55	0.923
12	6.86	3.43	37	2.52	1.570	2.550	5.00	3.28	6.67	0.938
13	7.84	4.41	38	2.52	1.400	2.550	5.66	3.27	7.55	0.945
14	9.80	6.37	38	2.52	1.280	2.550	7.33	3.26	9.77	0.949
15	11.76	8.33	38	2.52	1.060	2.550	8.83	3.24	11.77	0.958
16	4.90	1.47	36	4.25	3.290	4.250	3.08	3.30	4.11	0.922
17	6.86	3.43	37	4.20	2.350	4.290	4.33	3.29	5.77	0.945
18	7.84	4.41	38	4.20	2.130	4.240	5.20	3.28	6.93	0.949
19	9.80	6.37	38	4.20	1.800	4.260	6.40	3.26	8.53	0.957
20	11.76	8.33	38	4.20	1.580	4.260	8.05	3.25	10.73	0.962
21	4.90	1.47	35	6.33	4.360	6.380	2.73	3.30	3.64	0.931
22	6.86	3.43	35	6.33	3.580	6.540	3.96	3.29	5.28	0.948
23	7.84	4.41	37	6.33	2.900	6.440	5.00	3.28	6.67	0.954
24	9.80	6.37	38	6.33	2.560	6.380	6.33	3.27	8.44	0.959
25	11.76	8.33	38	6.33	2.650	6.530	7.81	3.25	10.41	0.969

recorded and the sum of these two flow rates was taken as the feed rate which is fixed at 20 LPM. Experimental runs were conducted by varying the feed concentration in the range of 0.690×10^{-3} to 6×10^{-3} kmol/m^3 (85–750 ppm) and feed pressure in the range of 2–13 atm (200–1200 KPa). For each set of feed concentration and feed pressure readings, the steady-state readings of permeate flow rate, retentate flow rate, permeate concentration and retentate concentrations were recorded. Permeate and retentate concentrations were measured by collecting the permeate and retentate and analyzing the samples using HPLC. A total of 25 sets of readings collected during these experimental runs are given in Table 2.

3. Theory

3.1. Model equations

The spiral-wound RO module in which the spatial variations of concentration and pressure on permeate and retentate sides were neglected is represented in Fig. 2. The concentration of solute

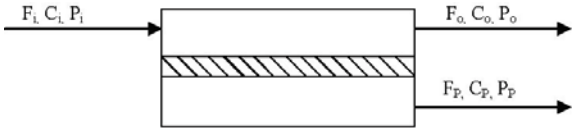

Fig. 2. Schematic representation of a spiral-wound module.

on the retentate side is considered to be uniform and equal to the outlet concentration C_o. Similarly, the uniform concentration of the solute on the permeate side is equal to the outlet permeate concentration C_p. The transmembrane pressure P, which is again uniform through the membrane, is taken to be

$$\Delta P = \left[\left(P_i + P_o\right)/2\right] - P_p \tag{1}$$

Due to the effect of concentration polarization [32], the concentration of solute at the membrane wall on the retentate side of the membrane C_w is related to the bulk concentration C_o by

$$e^{\left(\frac{J_v}{k}\right)} = \frac{C_w - C_p}{C_o - C_p} \tag{2}$$

where J_v is the solvent flux ($m^3/s.m^2$) and k is the mass transfer coefficient (m/s).

The ratio of C_w to C_o is defined as the polarization modulus M:

$$M = C_w / C_o \tag{3}$$

Assuming the solution–diffusion model, the transport equations for the solute and solvent (water) are expressed by the following equations.

$$J_s = B_s\left(C_w - C_p\right) \tag{4}$$

$$J_v - A_w\left(\Delta P - \Delta\Pi\right) \tag{5}$$

$$J_s = J_v C_p \tag{6}$$

where J_s is the solute flux (kmole/m^2.s), A_w is the solvent transport parameter [m/(s.atm)], B_s is the solute transport parameter (m/s), and $\Delta\Pi$ is the osmotic pressure difference across the membrane in atm. Here,

$$\Delta\Pi = \Pi\left(\mathrm{C_w}\right) - \Pi\left(\mathrm{C_p}\right) \tag{7}$$

where $\Pi(C)$ is the osmotic pressure at the solute concentration C. Taking $\Pi(C)$ to be linearly dependent on C, $\Pi(C)$ can be written as

$$\Pi(C) = K_o C \tag{8}$$

where K_o is the osmotic coefficient (atm m^3/mol). For an ideal solution that obeys the Van't Hoff relation, the osmotic pressure is $\Pi = RTC$ and the osmotic coefficient is $K_o = RT$ (R = universal gas constant, 8314 J $kmol^{-1}$ K^{-1}). Thus, the osmotic coefficient can be considered as a linear function of temperature and written as

$$K_o = \gamma T$$

where $\gamma = R$ for the ideal solution. Therefore,

$$\Pi(C) = \gamma TC \tag{9}$$

And hence Eq. (7) becomes

$$\Delta\Pi = \gamma T\left(C_w - C_p\right) \tag{10}$$

Defining the rejection coefficient R, the intrinsic rejection coefficient R^0, the cut θ and separation coefficient α as

$$R^0 = 1 - \left(\frac{C_p}{C_w}\right) \tag{11}$$

$$R = 1 - \left(\frac{C_p}{C_o}\right) \tag{12}$$

$$\theta = \frac{F_p}{F_i} \tag{13}$$

$$\alpha = A_w / B_s \tag{14}$$

The following equations hold good:

$$M = \frac{e^{\frac{J_v}{k}}}{R^o + \left(1 - R^o\right).e^{\frac{J_v}{k}}} \tag{15}$$

$$C_o = \frac{C_i}{(1-\theta) \; + \; \theta \, M \; \left(1 - \; R^o\right)} \tag{16}$$

$$C_p = MC_o\left(1 - R^o\right) \tag{17}$$

$$J_v = B_s \left(\frac{R^o}{1 - R^o}\right) \tag{18}$$

$$R^o = \frac{\alpha(\Delta P - \Delta\Pi)}{1 + \alpha(\Delta P - \Delta\Pi)} \tag{19}$$

Flux J_v and permeate flow rate F_p are related by

$$J_v = F_p / A_m \tag{20}$$

The equations listed above constitute the mathematical model of the spiral-wound RO module. The model has four parameters, namely A_w, B_s, k and γ. Knowing the values of these parameters, the mathematical model can be used to predict the rejection coefficients R for any given feed concentration C_i, transmembrane pressure P and feed temperature T. This calculation involves the following iterative steps

- Step 1: Assume R^0. Initial guess:

$$R^0 = \frac{\alpha\Delta P}{1 + \alpha\Delta P}$$

- Step 2: Calculate J_v using Eq. (18)
- Step 3: Calculate F_p using Eq. (20)
- Step 4: Calculate M using Eq. (15)
- Step 5: Calculate θ using Eq. (13)
- Step 6: Calculate C_o using Eq. (16)
- Step 7: Calculate C_p using Eq. (17)
- Step 8: Calculate C_w from Eq. (3)
- Step 9: Calculate Π from Eq. (10)
- Step 10: Calculate R^0 using Eq. (19)
- Step 11: Compare the calculated value of R^0 with the assumed value
- Step 12: Go to step 1 and repeat until the assumed R^0 is equal to the calculated R^0.
- Step 13: Calculate $R = 1 - (C_p/C_o)$.

3.2. Parameter estimation

Parameters of any model are generally estimated by fitting the experimental data with the values predicted by the model. This is done either by using a rigorous least square optimization technique or by a graphical method if the model equations can be expressed in a linear form. In this work, a graphical approach for the estimation of model parameters is used. Parameters B_s and k are estimated using the method proposed by Murthy and Gupta. [30]. They have shown that the equation for the RO system can be written as

$$\ln\left[\frac{J_v.(1-R)}{R}\right] = \frac{J_v}{k} + \ln B_s \tag{21}$$

Using the above equation, the parameters B_s and k (which is a constant value for fixed feed flow rate) can be estimated by plotting

$$\ln\left[\frac{J_v.(1-R)}{R}\right]$$

vs. J_v and equating the slope to $1/k$ and intercept to ($\ln B_s$) of the best linear fit.

A graphical method is proposed here for estimation of the other two parameters A_w and γ from the experimental data. Substituting Eqs. (4), (6) and (10) in Eq. (5) and rearranging the terms, the following equation is obtained:

$$TC_p = \frac{B_s}{\gamma}.\left[\frac{\Delta P}{J_v}\right] - \frac{1}{\gamma}.\left[\frac{B_s}{A_w}\right] \quad (22)$$

It is clear from the above equation that a plot of TC_p vs. $\Delta P/J_v$ is a linear plot with a slope equal to B_s/γ and an intercept equal to $-1/\gamma\cdot(B_s/A_w)$. The values of the other two parameters of the model A_w and γ are obtained by making a linear fit of the data points on the plot of

$$TC_p \text{ vs. } \frac{\Delta P}{J_v}$$

4. Results and discussion

The experimental data were obtained for a dimethylphenol–water–polyamide system at operating pressures ranging from 2 to12 atm and feed concentrations in the range of 85–750 ppm. The rejection coefficient is observed to vary between 92% to 97% for the transmembrane pressure and feed concentrations selected in this study. The minimum rejection of 92.25% is obtained for 2.52×10^{-3} kmol/m^3 feed concentration at 3.185 atm transmembrane pressure and maximum rejection of 97% is observed for 6.33×10^{-3} kmol/m^3 at 10.045 atm transmembrane pressure. The effect

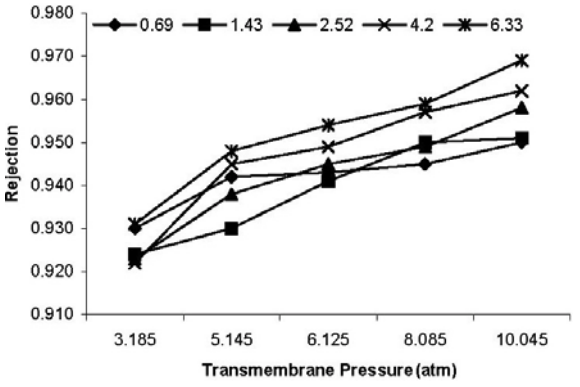

Fig. 3. Rejection vs. transmembrane pressure for various feed concentrations, $C_i\times10^{+3}$ (kmol/m^3) of dimethyl phenol.

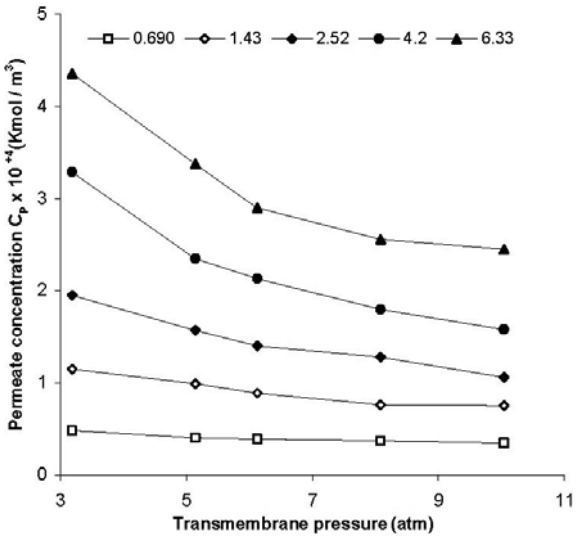

Fig. 4. Permeate concentration vs. transmembrane pressure at various feed concentrations, $C_i\times10^{+3}$(kmol/m^3) for dimethyl phenol.

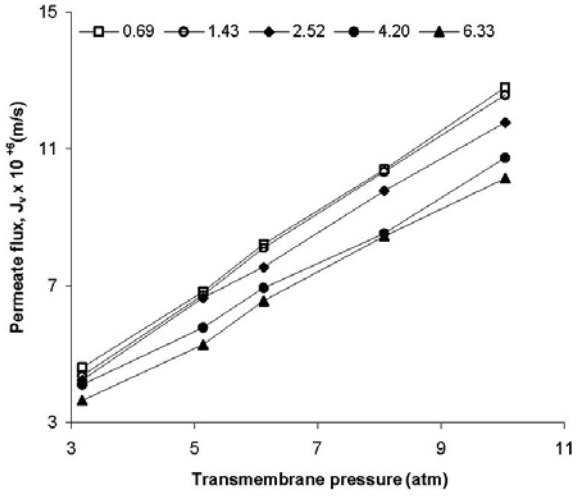

Fig. 5. Permeate flux vs. transmembrane pressure at various feed concentrations, $C_i\times10^{+3}$ (kmol/m^3) for dimethyl phenol.

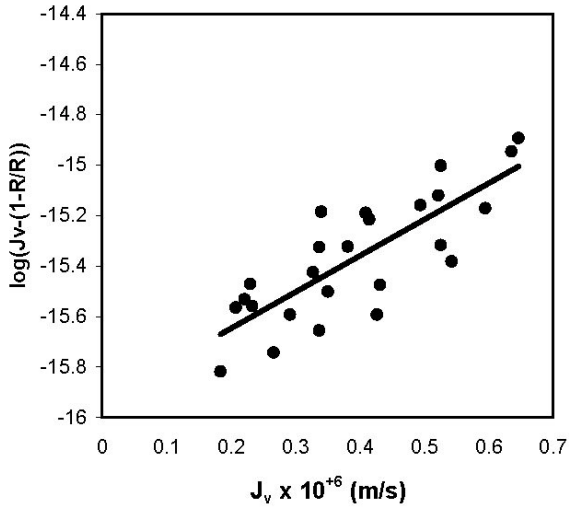

Fig. 6. Graphical plot for the estimation of parameters B_s and k.

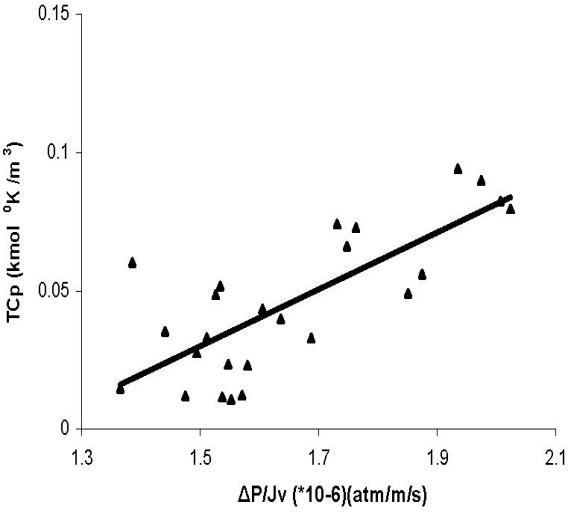

Fig. 7. Graphical plot for the estimation of parameters A_w and γ.

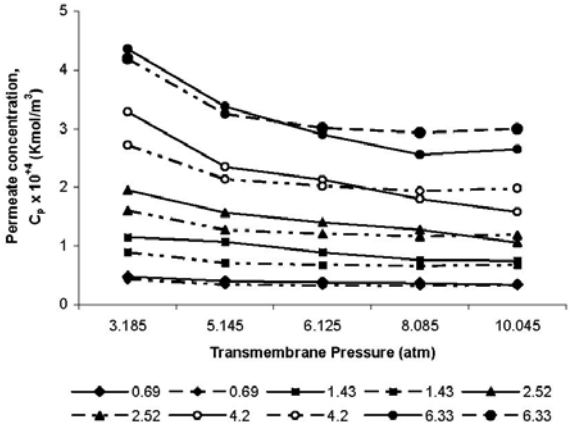

Fig. 8. Permeate concentration vs. transmembrane pressure for various feed concentrations. Comparison of experimental data (thick lines) and theoretical data (dotted lines).

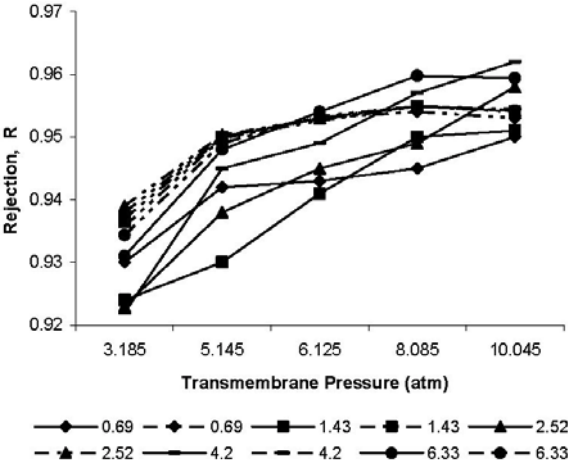

Fig. 9. Rejection vs. transmembrane pressure for various feed concentrations. Comparison of experimental (thick lines) and theoretical (dotted lines) data.

of transmembrane pressure on rejection, outlet permeate concentration and permeate flux for different feed concentrations is shown in Figs. 3–5, respectively. It is clear from these figures that for all feed concentrations, the rejection and permeate flux increase with transmembrane pressure and permeate concentration decreases with transmembrane pressure. These trends are in expected lines. From Fig. 4, it is observed that for any given ΔP, the permeate concentration increases with feed concentration. From Fig. 3, the rejection also shows a similar trend of increase in feed concentration for a particular pressure. However, permeate flux decreases with feed concentration for any particular ΔP as seen in Fig. 5. The osmotic pressure difference $\Delta\Pi$ increases

Table 3
Estimated model parameters

Parameter	Value
Solvent transport parameter (A_w), m/(s.atm)	8.6428×10^{-7}
Solute transport parameter (B_s), m/s	1.1822×10^{-7}
Mass transfer coefficient (k), m/s	6.7848×10^{-6}
Osmotic pressure factor (atm K/m^3 kmole)	1.1702

with increase in feed concentration. This results in a decrease in the driving force $\Delta P - \Delta\Pi$ for the permeation of solvent across the membrane. So, permeate flux decreases with increase in feed concentration as observed in Fig. 5. However, this trend is prominently visible only at concentrations higher than 150 ppm.

The plots of

$$\left[\frac{J_v(1-R)}{R}\right]$$

Table 4
Experimental and theoretical data showing permeate and rejection characteristics for dimethyl phenol separation

Set no.	ΔP, atm	$C_i\times10^{+3}$, kmol/m^3	$C_p\times10^{+4}$, kmol/m^3		% Error	Rejection ratio (R)		% Error
			(Exp)	(Theo)		Exp	Theo	
1	3.185	0.690	0.486	0.430	11.52	0.930	0.938	−0.87
2	5.145	0.690	0.402	0.345	14.18	0.942	0.950	−0.89
3	6.125	0.690	0.389	0.329	15.42	0.943	0.953	−0.99
4	8.085	0.690	0.379	0.320	15.55	0.945	0.954	−1.04
5	10.045	0.690	0.348	0.329	5.45	0.950	0.953	−0.42
6	3.185	1.430	1.150	0.939	18.35	0.924	0.937	−1.40
7	5.145	1.430	1.070	0.971	9.25	0.930	0.950	−2.16
8	6.125	1.430	0.890	0.784	11.87	0.941	0.953	−1.21
9	8.085	1.430	0.760	0.663	12.74	0.950	0.954	−0.45
10	10.045	1.430	0.750	0.681	9.20	0.951	0.954	−0.26
11	3.185	2.520	1.950	1.605	17.65	0.923	0.936	−1.49
12	5.145	2.520	1.570	1.274	18.82	0.938	0.950	−1.27
13	6.125	2.520	1.400	1.210	13.54	0.945	0.953	−0.84
14	8.085	2.520	1.280	1.168	8.70	0.949	0.954	−0.54
15	10.045	2.520	1.060	1.195	−12.79	0.958	0.954	0.44
16	3.185	4.200	3.290	2.723	17.23	0.922	0.935	−1.44
17	5.145	4.200	2.350	2.143	8.79	0.945	0.949	−0.49
18	6.125	4.200	2.130	2.029	4.72	0.949	0.952	−0.31
19	8.085	4.200	1.800	1.948	−8.25	0.957	0.954	0.30
20	10.045	4.200	1.580	1.642	− 3.97	0.962	0.954	0.88
21	3.185	6.330	4.360	4.193	3.83	0.931	0.934	−0.30
22	5.145	6.330	3.580	3.257	9.02	0.948	0.949	−0.12
23	6.125	6.330	2.900	3.018	−4.09	0.954	0.953	0.17
24	8.085	6.330	2.560	2.935	−14.67	0.959	0.954	0.51
25	10.045	6.330	2.650	3.001	−13.26	0.969	0.954	1.54

vs. J_v and TC_p vs. $\Delta P/J_v$ were drawn and are shown in Figs. 6 and 7. The model parameters, namely A_w, B_s, k and γ were estimated from the above-mentioned plots as explained in Section 3.2. The estimated values of the model parameters are given in Table 3. Using the estimated parameter values in the model equations (Section 3.1), the theoretical values of rejection coefficient and permeate concentration were calculated and compared with the experimental values. The comparison of predicted and experimental values is given in Table 4 and also shown in Figs. 8 and 9. The model is able to predict the permeate concentration within an error of 19% and rejection within 2% error. This validates the lumped parameter model and the parameter estimation techniques reported in this work.

5. Conclusions

Experimental studies were conducted on a laboratory-scale spiral-wound RO membrane module to study the rejection efficiency of polyamide membranes in separating a dimethyl phenol water system. By varying the P between 2 to 12 atm and the feed concentration from $0.69l\times10^{-3}$ kmol/m^3 to 6.33×10^{-3} kmol/m^3 (85–750 ppm), the rejection coefficient values of the membrane were measured and found to vary from 92% to 97%.

A lumped parameter model for the spiral-wound RO module was developed assuming the solution–diffusion mechanism with concentration polarization for solute and solvent transport through the membrane. The model has four parameters, namely A_w, B_s, k and γ. A graphical procedure was used to estimate the model parameters by fitting the experimental data with the model equations. In addition to using the method proposed by Murthy and Gupta [30] for the estimation of two of the four parameters (B_s and k), a new method is also proposed in this work for estimating the remaining two parameters (A_w and γ). The model and the estimated parameter values were validated with the experimental data and the model is able to predict the permeate concentration and rejection within an error of 19% and 2% respectively.

6. Symbols

A_m — Membrane area, m^2
A_w — Solvent transport parameter, m/atm. s
B_s — Solute transport parameter m/s
C — Concentration of solute, kmol of solute per m^3 of solution
C_i — Concentration of solute in feed, kmol of solute per m^3 of solution
C_o — Concentration of solute in retentate, kmol of solute per m^3 of solution
C_p — Concentration of solute in permeate, kmol of solute per m^3 of solution
C_w — Concentration of solute at membrane wall, kmol of solute per m^3 of solution
F_i — Feed flow rate, m^3/s
F_o — Retentate flow rate, m^3/s
F_p — Permeate flow rate, m^3/s
J_s — Solute flux, kmole/m^2.s
J_v — Solvent flux, m^3/m^2.s
k — Mass transfer coefficient, m/s
K_o — Osmotic pressure coefficient, atm m^3/kmol
M — Concentration modulus
P — Pressure, atm
P_i — Pressure in the feed inlet, atm
P_o — Pressure in the retentate side, atm
P_p — Pressure in the permeate side, atm
R — Rejection coefficient
R^0 — Intrinsic rejection coefficient
T — Temperature, K

Greek

α — Separation coefficient, atm^{-1}
Δ — Difference across the membrane

γ — Osmotic pressure factor, atm K/m^3 kmol

Π — Osmotic pressure, atm

Acknowledgement

This research work was supported by a TAPTEC project grant from the All India Council of Technical Education (AICTE), New Delhi.

References

[1] P. Hillis, Membrane Technology in Waste and Waste Water Treatment, Royal Society of Chemistry, Cambridge, 2000.

[2] S. Sourirajan and T. Matsuura, Reverse osmosis/ ultrafiltration process principles, National Research Council Canada, Ottawa, 1985, pp. 848–884.

[3] C.S. Slater, R.C. Ahlert and C.G. Vahrin, Reverse osmosis processes for the renovation and reuse of hazardous industrial wastewaters, Current Proc. Environ. Eng., 3 (1987) 1–13.

[4] C.S. Slater, R.C. Ahlert and C.G. Uchrin, Applications of reverse osmosis to complex industrial wastewater treatment, Desalination, 48 (1983) 171–187.

[5] A.J. Shuckrow, A.P. Pajak and J.W. Osheke, EPA–600/2-81-019, 1981.

[6] A.J. Shuckrow, A.P. Pajak and C.J. Touhill, EPA – 600/2-81-019, 1980.

[7] Y. Yoon, P. Westerhoff, S.A. Synder and E.C. Wert, Nanofiltration and ultrafiltration of endocrine disrupting compounds, Pharmaceuticals and personal care products, J. Membr. Sci., 270 (2006) 88–100.

[8] K. Kimura, S. Toshima, G. Amy and Y. Watanabe, Rejection of neutral endocrine disrupting compounds (EDCs) and pharmaceutical active compounds (PhAc) by RO membranes, J. Membr. Sci., 245 (2004) 71–78.

[9] Y.Yoon and R.M. Lupetow, Removal of organic contaminants by RO and NF membranes, J. Membr. Sci., 261 (2005) 76–86.

[10] A. Bodalo-Santoyo, J.L. Gomez-Carasco, E. Gomez-Gomez, M.F. Maximo-Martin and A.M. Hidalgo-Montesinos, Application of reverse membrane to reduce pollutants present in industrial waste water, Desalination, 155 (2003) 101–108.

[11] S. Sourirajan and T. Matsuura, Physicochemical criteria for reverse osmosis separation of alcohols, phenols, and monocarboxylic acids in aqueous solutions using porous cellulose acetate membranes, J. Appl. Polym. Sci., 15 (1971) 2905–2927.

[12] H.K. Lonsdale, U. Merten and M. Tagami, Phenol transport in cellulose acetate membranes, J. Appl. Polym. Sci., 11 (1967) 1807–1820.

[13] S. Sourirajan., T. Matsuura, P. Blais and J.M. Dickson, Reverse osmosis separations for some alcohols and phenols in aqueous solutions using aromatic polyamide membranes, J. Appl. Polym. Sci., 18 (1974) 3671–3684.

[14] S. Sourirajan, T. Matsuura and M.E. Bednas, Reverse osmosis separation of single and mixed alcohols in aqueous solutions using porous cellulose acetate membranes, J. Appl. Polym. Sci., 18 (1974) 567–588.

[15] T. Matsuura, Y. Fang and S. Sourirajan, Reverse osmosis separation of binary organic mixtures using cellulose acetate butyrate and aromatic polyamide membranes, J. Appl. Polym. Sci., 44 (1992) 1959–1969.

[16] C.F. Schutte, The rejection of specific organic compounds by reverse osmosis membranes, Desalination, 158 (2003) 285–294.

[17] A. Bodalo-Santoyo, J.L. Gomez-Carasco, E. Gomez-Gomez, M.F. Maximo-Martin and A.M. Hidalgo-Montesinos, Spiral-wound membrane reverse osmosis and the treatment of industrial effluents, Desalination, 160 (2004) 151–158.

[18] V.V. Goncharuk, D.D. Kucheruk, V.M. Kochkodan and V.P. Badekha, Removal of organic substances from aqueous solutions by reagent enhanced reverse osmosis, Desalination, 143 (2002) 45–51.

[19] H.K. Lonsdale, U. Merten and R.L. Riley, Transport properties of cellulose acetate osmotic membranes, J. Polym. Sci., 9 (1965) 1341–1362.

[20] O. Kedem and K.S. Spiegler, Thermodynamics of hyperfiltration (reverse osmosis): Criteria for efficient membranes, Desalination, 1 (1966) 311–326.

[21] R. Rautenbach and R. Albrecht, Membrane Processes, Wiley, New York, 1989.

[22] M. Sultanieh and W.N. Gill, Review of reverse

osmosis membranes and transport models, Chem. Eng. Comm., 12 (1981) 279–363.
[23] J.L. Marriott, E. Sorensen and I.D.L. Bogle, Detailed mathematical modeling of membrane modules, Comp. Chem. Eng., 25 (2001) 693–700.
[24] H.G. Burghoff, K.L. Lee and W. Pusch, Characterization of transport across cellulose acetate membranes in the presence of strong solute—membrane interactions, J. Appl. Polym. Sci., 25 (1980) 323–347.
[25] S. Kimura and S. Sourirajan, Analysis of data in reverse osmosis with porous cellulose membranes used, AIChE J., 13 (1967) 497–503.
[26] J. Marriott and E. Sorensen, A general approach to modeling membrane modules, Chem. Eng. Sci., 58 (2003) 4975–4990.
[27] K.K. Sirkar and P.T. Dang, Approximate design equations for reverse osmosis desalination by spiral-wound modules, Ind. Eng. Chem. Process Des. Dev., 21 (1982) 517–527.
[28] S. Senthilmurugan, A. Ahluwalia and S.K. Gupta, Modeling of a spiral-wound module and estimation of model parameters using numerical techniques, Desalination, 173 (2005) 269–286.
[29] F. Evangelista and G. Jonsson, Optical design and performance of spiral wound modules I: Numerical method, Chem. Eng. Comm., 72 (1988) 69–81.
[30] Z.V.P. Murthy and S.K. Gupta, Sodium cyanide separation and parameter estimation for reverse osmosis thin film composite polyamide membrane, J. Membr. Sci., 154 (1999) 89–103.
[31] Z.V.P. Murthy and S.K. Gupta, Estimation of mass transfer coefficient using a combined nonlinear membrane transport and film theory model, Desalination, 109 (1997) 39–49.
[32] P.C. Wankat, Rate-controlled Separations, Springer International, 1994.